IL NUOVO CIMENTO Vol. 27 C, N. 6 Novembre-Dicembre 2004
DOI 10.1393/ncc/i2003-10021-9

Natural solar energy amplifiers in planet-atmosphere systems(*)

E. C. Njau

Physics Department, University of Dar es Salaam - P.O. Box 35063, Dar es Salaam, Tanzania

(ricevuto il 16 Settembre 2003; revisionato l'1 Febbraio 2005; approvato l'11 Febbraio 2005)

Summary. — Planets and their atmospheres (including the Earth and its atmosphere) continuously receive solar energy which comprises very small variable components and a relatively huge constant component. On the basis of certain conditions, specific physical mechanisms can exist in each planet-atmosphere system under which the tiny variable solar energy components so received apparently undergo large amplifications. In the case of the Earth-Atmosphere system, these energy amplifications continuously exist and involve maximum amplification factors that range from ~ 2312 to over 6915 for frequencies equal to or less than the 11-year sunspot cycle frequency. Consequently energy and hence temperature variations at the solar (or sunspot) cycle frequencies dominantly exist in the Earth-Atmosphere system. These energy and temperature variations are continuously mapped or translated into corresponding variations in the other weather parameters as verified by past records.

PACS 96.30.-t – Planets, their satellites and rings; asteroids.
PACS 92.60.Ry – Climatology.
PACS 96.40.Kk – Solar modulation and geophysical effects.

1. – Introduction

In a very simplified form, a single-stage amplifier in an electronic system can be represented by fig. 1. Here signal A_0 is usually an electric current and signal a_0 is usually an electric current or voltage, all of which are supplied by the battery or power supply that is powering the amplifier. The amplifying device is a transistor or a vacuum tube, and signal V_i is of similar form as signal a_0 except that the former is variable. Let us suppose that the free end of the movable arm R is now hooked onto Q, allowing the small input signal V_i to enter into the amplifying device. What this device does is to make a large part of signals A_0 and V_0 oscillate at the frequency of the relatively small signal V_i (*e.g.*, see ref. [1] for details). Consequently the output signal V_0 contains amplified versions of the input signal V_i. The output signal V_0 is fed into a load. Here, a

(*) The author of this paper has agreed to not receive the proofs for correction.

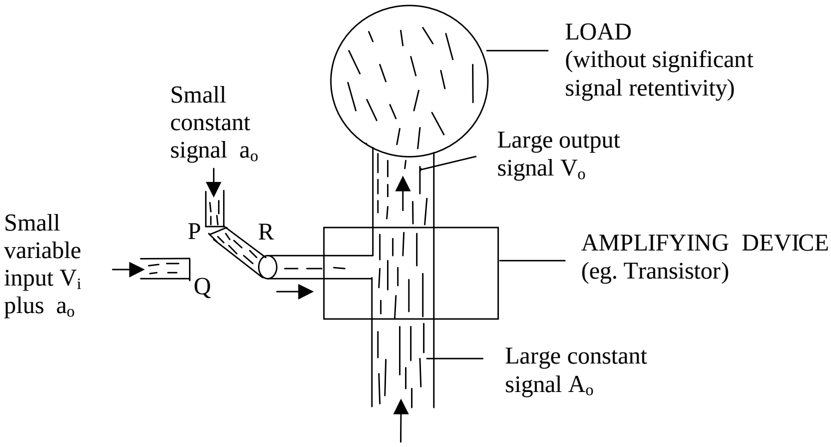

Fig. 1. – Simplified representation of a single-stage electronic amplifier. This amplifier is man-made and hence does not exist naturally.

load is a structure or system into which the output signal is delivered. The account given above summarises in a simple manner how an electronic amplifier works. This amplifier is man-made and hence is not natural.

The aim of this paper is to find out and establish whether natural energy amplifiers can or do exist on/over the Earth and the other planets. Conceptually if such a natural amplifier exists, it would possibly take the form illustrated in fig. 2. Here the term "load" represents a planet together with its atmosphere. The only significant energy signals which are fed onto the planet and its atmosphere are the large constant component of

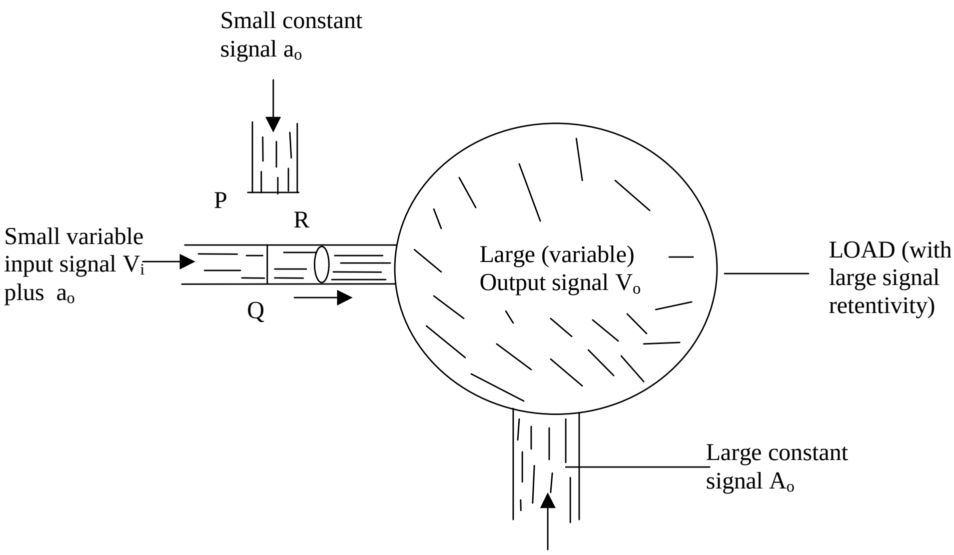

Fig. 2. – Simplified representation of a single-stage amplifier that can possibly exist naturally, *e.g.*, in a planet-atmosphere system.

incident solar energy and the small variable component of incident solar energy. In this case there is no amplifying device, and both the input signal V_i and the constant signal $(a_0 + A_0)$ are fed directly into the load. Amplification would take place if a large part of $(a_0 + A_0)$ is made to oscillate at the frequency of the relatively small signal V_i. It is apparent that if a large part of $(a_0 + A_0)$ is to be made to oscillate at the frequency of V_i, then such an amplifying process can only be done through the (free) interactions of the signals in the load. Since the frequencies of the tiny variable components of earthward solar energy are significantly reflected in past climate records [2-5], we suspect or hypothesize that there might be an important amplifying process in a typical planet-atmosphere system in respect of the tiny variable components of incident solar energy. In the following section we prove that such an amplifying process actually takes place in the Earth-Atmosphere system as well as on/over some other planets. In other words, this proof establishes existence of natural energy amplifiers.

2. – Analysis

2·1. *General derivation.* – Let us consider fig. 2 and assume that the free end of the movable arm R is hooked permanently at Q. In this case there is no amplifying device. But the load present is special in that it has non-zero signal retentivity. Hence any resulting signal amplification would be due to free signal interactions. Now the load (*i.e.* planet-atmosphere system) receives large constant signal $A = A_0 + a_0$ and small variable signal $V_i = s_1(t) + s_2(t) + \dots\dots\dots + s_N(t)$, where $s_n(t)$ is the n-th variable component in V_i, N is a positive integer, and t represents time. Over a period less than few thousand years, the solar energy stream incident upon the above-mentioned planet-atmosphere system (PAS) consists of a huge constant component A and N relatively tiny variable components $s_1(t)$, $s_2(t), \dots\dots\dots, s_N(t)$ such that these tiny variable components make up V_i. Let us select arbitrarily one of these N variable components and call it or refer to it as $c(t)$, and also assume that this particular component has amplitude d_0 and frequency f_0. If $E(t)$ represents the total solar energy stream incident on the PAS, then

$$E(t) = A + c(t) + [N - 1 \text{ variable components}] \,. \tag{1}$$

What follows is that an analysis on $A + c(t)$ is first done, and later on the remaining $N - 1$ variable components shown in eq. (1) will be finally taken into account in order to make the analysis complete by making it apply over the whole $E(t)$.

As a starting point, focus is put on how $A + c(t)$ is processed into the PAS. The net portion of $A + c(t)$ which is absorbed into the PAS from $t = 0$ up to $t = T$ (*i.e.* over observation time T) is denoted by $D_T(t)$ and given as

$$D_T\,(t) = [A + c(t)]g\,(t) - R\,(t)\ , \tag{2}$$

where $g(t)$ = stretch of $[1 -$ PAS albedo$]$ from $t = 0$ to $t = T$ (*i.e.* over observation time T) and $R(t)$ is energy radiated from the PAS to space through long-wave or terrestrial radiation from $t = 0$ to $t = T$ (*i.e.* over observation time T). Let $s(t) = A + c(t)$ and also let $S(f)$, $G(f)$, $L(f)$ and $M_T(f)$ represent, respectively, the frequency spectra of $s(t)$, $g(t)$, $R(t)$ and $D_T(t)$ such that f denotes frequency. It is obvious that

$$M_T\,(f) = G\,(f) * S\,(f) - L(f)\,, \tag{3}$$

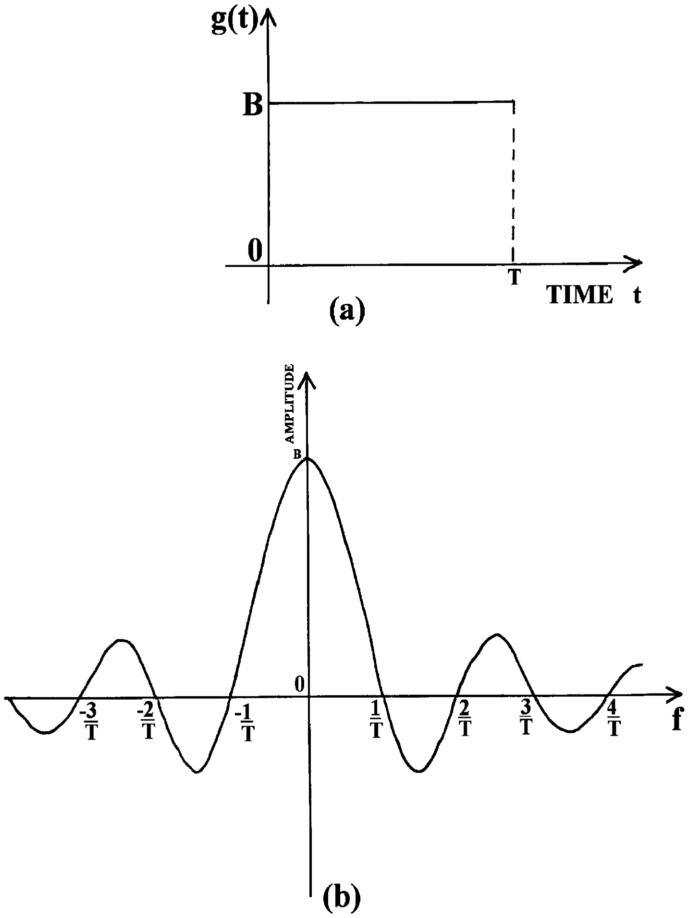

Fig. 3. – Graphical representation of: (a) $g(t)$ *vs.* time t, and (b) [amplitude spectrum of $g(t)]/e^{-j\pi fT}$ *vs.* frequency f.

where "$*$" denotes convolution operation. If the average value of $g(t)$ is assumed to be B, then a plot of $g(t)$ *vs.* t and that of $G(f)/e^{-j\pi fT}$ *vs.* f are given in figs. 3(a) and (b), respectively. Also graphical plots of $s(t)$ and $S(f)$ are given in figs. 4(a) and (b), respectively. Since convolution operation has a distributive property, then

$$
\begin{aligned}
(4) \qquad G(f) * S(f) &= S(f) * \sum_{f} \{\text{value of } G(f) \text{ at individual frequency}\} \\
&= S(f) * [G(f_1) + G(f_2) + \ldots\ldots\ldots] \\
&= S(f) * G(f_1) + S(f) * G(f_2) + \ldots\ldots\ldots
\end{aligned}
$$

Suppose we choose a specific point Y on the frequency spectrum structure in fig. 3(b) and assume that the frequency at this point Y at time t is denoted by F_t. It is obvious that F_t is T-dependent and is also "attached" to the point Y which is itself attached onto the G-structure in fig. 3(b). As T increases both point Y on the G-structure and F_t

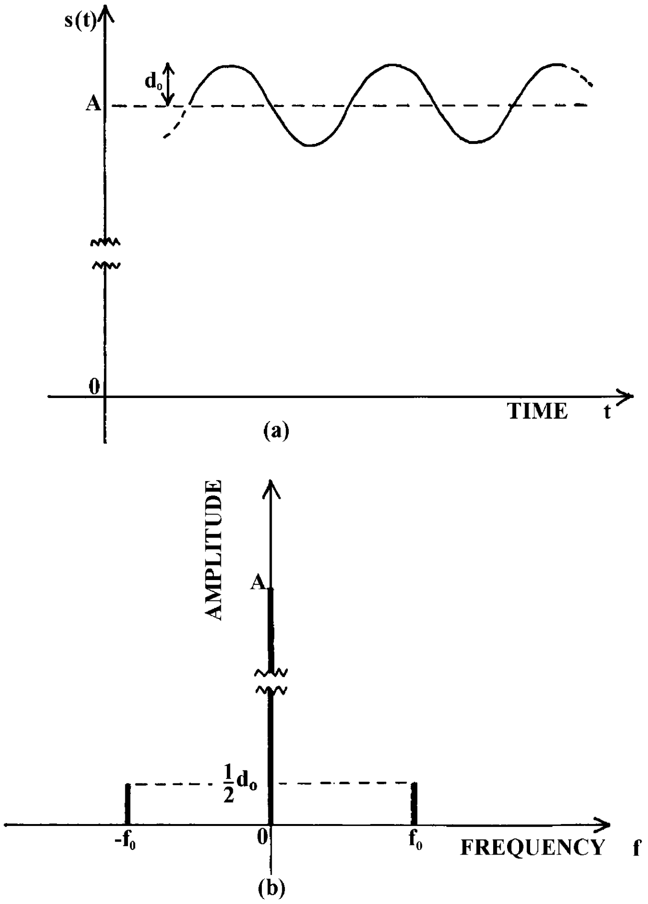

Fig. 4. – Graphical representation of: (a) $s(t)$ *vs.* time t, and (b) [the amplitude spectrum of $s(t)$] *vs.* frequency f.

(in figs. 3(b) and 5) would drift towards lower frequencies along the horizontal frequency axis. Let us suppose that $G(F_t) = b$ such that b is not too small. Then a plot of $S\left(f\right) * G\left(F_t\right)/e^{-j\pi fT}$ *vs.* f is shown in fig. 5 for positive values of f. The length of the observation time T starts from 24 hours and proceeds upwards. As t and hence observation time T increase, the three vertical lines in fig. 5 at $f = F_t - f_0$, $f = F_t$ and $f = F_t + f_0$ gradually move together towards the point $f = 0$. Let the frequency spectrum structure in fig. 5 at time t be represented by $X_T(t)$. Since the three lines just mentioned are spectrally tied together, they inevitably move together at common speed. This collective motion takes place continuously with time, and the only occasion when this motion stops temporarily is when the vertical line at $f = F_t - f_0$ reaches the point $f = 0$, that is, $F_t = f_0$. This temporary stoppage is inevitable because according to standard signal processing theory (*e.g.*, see refs. [6, 7]), the vertical line at $f = F_t - f_0$ cannot cross point $f = 0$ and move into negative values of f. Instead, it stops at $f = 0$ before starting motion in the reverse direction (*i.e.* towards the right-hand side of fig. 5).

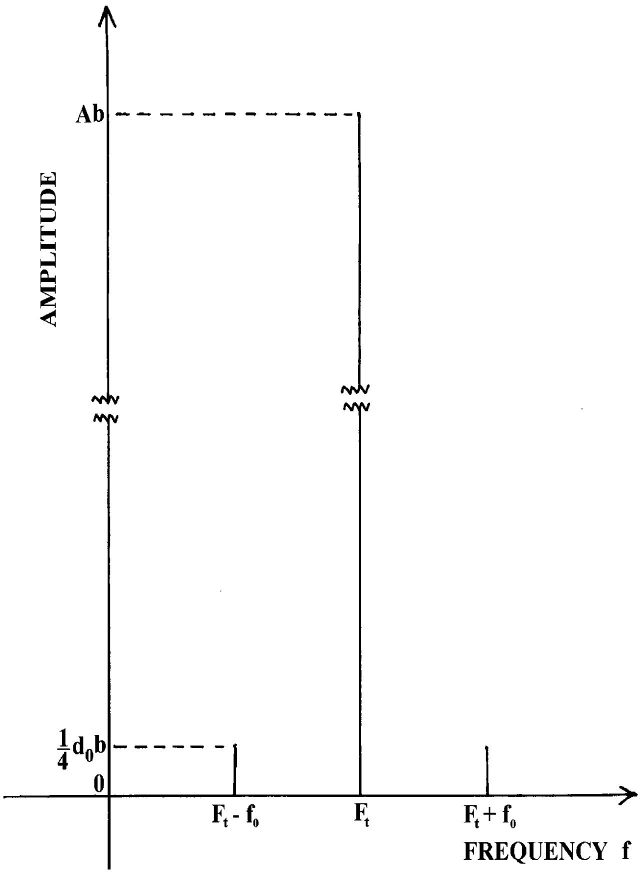

Fig. 5. – Graphical representation of $[S(f) * G(F_t)/e^{-j\pi fT}]$ *vs.* frequency f.

That is, the condition

$$\frac{\mathrm{d}X_T\,(t)}{\mathrm{d}t} = 0 \tag{5}$$

holds for sometime only when $F_t = f_0$. What physically happens when $\mathrm{d}X_T(t)/\mathrm{d}t = 0$ is that all the frequency spectrum structures in fig. 5 stay at non-changing frequencies by having their spatial velocities change proportionally with their wavelengths since: Velocity = Frequency × Wavelength. At the same time, the structures at frequency $F_t - f_0$ that had frequency-decreasing trends when F_t was greater than f_0 are converted to other structures with frequency-increasing trends. This conversion process is completed when the magnitudes of the created (velocity)/(wavelength) patterns start increasing with time. It is easy to justify eq. (5) under condition $F_t = f_0$ using basic laws of mechanics. A body moving along a straight line cannot reverse its motion along the same straight line without temporarily stopping at the reversing point. Similarly, the line at frequency $F_t - f_0$ cannot reverse its motion at point $F_t - f_0 = 0$ without stopping temporarily at this point. And during this temporary stoppage, a large amplitude Ab exists at frequency f_0. Remember that stoppage of the vertical line at frequency $F_t - f_0$

implies also stoppage of the vertical lines at frequencies F_t and $F_t + f_0$. This is because these 3 lines are spectrally tied together. Since the large peak at $f = F_t$ and height Ab stops and hence stays for a longer period at frequency f_0 than at any other frequency, $D_T(t)$ is characterized by large dominant oscillations at frequency f_0. And also since frequency F_t has been chosen arbitrarily, then consideration of all the other frequencies in $G(f)$ as we have done to F_t leads to existence of oscillations in $D_T(t)$ at frequency f_0 and amplitude $A\beta$, where β depends on the corresponding value of $G(f)$ at $f = f_0$ since the frequency structure of $G(f)$ changes with T. The curve in fig. 3(b) is represented by Amplitude $= BT\,\mathrm{sinc}(fT)$, where $\mathrm{sinc}(x) = \sin(\pi x)/\pi x$ (*e.g.*, see ref. [7]). Therefore the oscillations in $D_T(t)$ at frequency f_0 generally have an amplitude equal to

$$\frac{e^{-j\pi f_0 T} ABT \sin(\pi f_0 T)}{\pi f_0 T} - L(f_0)\,.$$

Referring back to fig. 2, we now have an input energy signal $c(t)$ at frequency f_0 and an output energy signal (in the PAS) with amplitude $\frac{e^{-j\pi f_0 T} ABT \sin(\pi f_0 T)}{\pi f_0 T} - L(f_0)$and frequency f_0. Here there is apparent energy amplification factor α_0 expressed as

$$\text{(6)} \qquad \begin{aligned}\text{Amplification factor } \alpha_0 &= \frac{\text{Amplitude of output energy signal}}{\text{Amplitude of input energy signal}}\\ &= \frac{AB}{f_0 d_0 \pi}[\sin(\pi f_0 T)]e^{-j\pi f_0 T} - \frac{L(f_0)}{d_0}\,.\end{aligned}$$

The inference given above has been arrived at by considering the constant component A and only one variable component $c(t)$. What conclusion will be arrived at if $c(t)$ and the remaining $N-1$ variable components $c_1(t)$, $c_2(t)$, $c_3(t), \ldots, c_{N-1}(t)$ are considered? Suppose we now consider the constant component A and all the N variable components and re-do the analysis. This is what would happen. First, fig. 4(a) would change by having the additional $N-1$ variable components superimposed upon line $s(t) = A$, noting that $s(t)$ is now equal to $E(t)$. Then fig. 4(b) would change by having N separate, vertical and short lines on either side of the vertical line $f = 0$. The vertical lines to the right-hand side of $f = 0$ would be at frequency f_0 and also at the frequencies f_1, f_2, f_3, $f_4, \ldots, f_{N-1}$ of $c_1(t)$, $c_2(t)$, $c_3(t)$, $c_4(t) \ldots, c_{N-1}(t)$, respectively. Second, figs. 3(a) and (b) remain unchanged. Third, fig. 5 would change by having N short vertical lines on either side of the vertical line at $f = F_t$. These short vertical lines would be at frequencies $F_t \pm f_0, F_t \pm f_1, F_t \pm f_2, \ldots F_t \pm f_{N-1}$. On this basis, the ensuring analysis would lead to the conclusion that

$$\text{(7)} \qquad M_T(t) = \sum_n \left[TAB\left(\frac{\sin(\pi f_n T)}{\pi f_n T}\right)e^{-j\pi f_n T} - L(f_n)\right],$$

where $n = 0, 1, 2, 3 \ldots, N-1$. Equation (7) above gives the amplitudes of the oscillations contained in $D_T(t)$.

We can now generally consider $c_n(t)$ as an input variable solar energy signal into the PAS at frequency f_n and amplitude a_n, where $n = 0, 1, 2, 3, 4 \ldots, N-1$. The corresponding output energy signal at frequency f_n can be obtained from eq. (7) such that the amplification factor α_n involved is given as

$$\alpha_n = \frac{\text{Amplitude of output energy signal}}{\text{Amplitude of input energy signal}} \tag{8}$$
$$= \frac{AB}{f_n a_n \pi} \left[\sin\left(\pi f_n T\right)\right] e^{-j\pi f_n T} - \frac{L\left(f_n\right)}{a_n}$$
$$= \frac{A'B}{f_n a'_n \pi} \left[\sin\left(\pi f_n T\right)\right] e^{-j\pi f_n T} - \frac{L\left(f_n\right)}{a_n}\,,$$

where A' and a'_n are the constant component and n-th variable component, respectively, of solar radiation power incident on the PAS per m^2. Since A and a_n apply over the whole cross-sectional area of the PAS, it is obvious that $A/a_n = A'/a'_n$.

According to the first law of thermodynamics, the PAS as a whole should be in radiative equilibrium averaged over a period of several years. In other words, as much energy must be leaving the PAS in the form of long-wave radiation as is entering in the form of short-wave radiation. Let us assume a case where a specific PAS (or large part thereof) has substantial heat storage capacity. Such a PAS will take several years to warm up from incident short-wave radiation so that there may be some reasonable time separation between the mainstream incident short-wave radiation pattern and the associated mainstream outgoing long-wave radiation pattern. In such a situation (which will be discussed further in the next section), the two expressions $\frac{L(f_n)}{a_n}$ and $\frac{A'B}{a'_n f_n \pi}[\sin(\pi f_n T)]e^{-j\pi f_n T}$ on the right-hand side of eq. (8) may be analysed or considered separately. Even aside from the argument just given, several authors (*e.g.*, see ref. [8]) treat/analyse the short-wave radiation expressions and long-wave radiation expressions separately when dealing with global radiation balance. The reasons for such separation are simple. First, short-wave radiation is unidirectional while long-wave radiation is thermal diffuse radiation. Second, the long-wave radiation is negligible at the wavelengths of short-wave radiation so that only absorption has to be considered in the case of short-wave radiation. Therefore, the short-wave radiation expressions in this paper may be analysed separately from the corresponding long-wave radiation expressions. On this basis, let us consider $c_n(t)$, for $n = 0, 1, 2, \ldots, N-1$ as tiny short-wave energy inputs into the PAS at frequencies f_n for $n = 0, 1, 2, \ldots, N-1$, respectively. Then these N input energy signals will give rise to shortwave-based energy oscillations $H_n(t)$ for $n = 0, 1, 2, \ldots, N-1$ in the PAS at frequencies f_n for $n = 0, 1, 2, ..., N-1$, respectively. On the basis of the analysis given earlier, $H_n(t)$ will be an amplified version of $c_n(t)$ and the amplification factor Ω_n involved is given as

$$\Omega_n = \frac{\text{Amplitude of } H_n(t)}{\text{Amplitude of } c_n(t)} \tag{9}$$
$$= \frac{A'B}{\pi f_n a'_n} \left[\sin(\pi f_n T)\right] e^{-j\pi f_n T}\,,$$

where a_n is the amplitude of $c_n(t)$. Consider the values of $A'B/\pi$ for the planets of the solar system given in table I, and since for all of the perturbations in the Earthward solar radiation due to the known solar or sunspot cycles [9, 10], $f_n a'_n \ll 1$, and hence eq. (9)

TABLE I. – *Tabulated values of $A'B$ and $\frac{A'B}{\pi}$ in eq.* (8) *for the planets in the Solar System.*

Name of planet	Value of B	Value of A' ($\mathrm{W/m^2}$)	Values of $A'B$ ($\mathrm{W/m^2}$) and corresponding $A'B/\pi$	
			$A'B$	$\frac{A'B}{\pi}$
1. Mercury	0.93	9079.1	8443.6	2689.0
2. Venus	0.24	2599.8	624.0	198.7
3. Earth	0.66	1360.0	897.6	285.9
4. Mars	0.85	586.0	498.1	158.6
5. Jupiter	0.55	50.2	27.6	8.8
6. Saturn	0.37	14.9	5.5	1.8
7. Uranus	0.37	3.7	0.5	0.2
8. Neptune	0.27	1.5	0.4	0.1
9. Pluto	0.84	0.9	0.8	0.3

represents very large amplification notably at

$$T = \frac{1}{2f_n}, \frac{3}{2f_n}, \frac{5}{2f_n}, \dots\dots\dots, \qquad \text{when} \quad \left|\sin(\pi f_n T)\, e^{-j\pi f_n T}\right| = 1\,.$$

Note that the values of B in table I have been calculated using corresponding albedo values from refs. [11, 12].

If we decide to start measuring the standard time t from the zero reference time shown in fig. 3(a), then we could generalize the observation time T and make it variable so that it increases together with t. In this case, the standard time is tied and equated to the observation time, that is, $T = t$. Under these conditions, eq. (9) may be written in the following form:

$$\Omega_n = \frac{A'B}{\pi f_n a'_n}[\sin(\pi f_n t)]e^{-j\pi f_n t}\,. \tag{10}$$

The assumptions under which eq. (9) changes to eq. (10) are realistic and natural because they include the condition that the PAS receives solar energy continuously, at least from the starting or reference time, irrespective of the researcher's observation time involved. Furthermore, these assumptions leave no room for conceptualizing that the PAS is denied solar energy at any duration, *e.g.*, by involving a single fixed step function. Note that eq. (10) mimics nature by being based on a variable step function which continuously expands with time t along the forward positive direction of time. As the step function expands with time, the perturbations leading to signal amplifications are repeated regularly at the basic system frequency f_n since Ω_n oscillates repetitively with time at frequency f_n. And the associated amplification represented by eq. (10) continues as long as there is a (small) variation in the solar constant at solar cycle frequency f_n. It is clear in this case that Ω_n is inversely proportional to the product $a_n f_n$. This fact is explained and commented upon in sect. **3**.

Further interpretation of eq. (10) reveals the following interesting feature. From just after 0 time to just before time $1/f_n$, approximately one cycle of an amplified and non-inverted energy signal at frequency f_n is set up. Then at time $1/f_n$, the signal at frequency f_n and all its harmonics are erased or cleared out of the PAS. Then from just after time $1/f_n$ up to just before time $2/f_n$, an amplified and inverted (*i.e.* phase-reversed) energy signal at frequency f_n is formed up to approximately one cycle. Then at time $2/f_n$, this signal and its harmonics are erased out of the PAS. Just after time $2/f_n$, an approximately one cycle of an enlarged and non-inverted energy signal at frequency f_n is set up, and then the alternating process just mentioned continues repeating itself indefinitely. This alternating process creates nonlinearities in the PAS which ultimately give rise to harmonics at frequencies $2f_n, 3f_n, \ldots$ etc. These harmonics also undergo phase reversal processes together with their fundamental oscillations. Furthermore, the alternating process makes sunspot cycles reflected in the PAS climate nonstationary in time. Such an alternating process (which is reflected in associated temperature variations) is illustrated in the next section in connection with the Earth's surface-atmosphere system.

Appropriate care must be taken when using eq. (8) and hence also the subsequent equations to make actual calculations. Application of all these equations must comply with the conditions on which fig. 3(a) is based. In other words, the units for T, A, a_n and f_n in the latter equations should be chosen in such a way that all significant albedo variations are averaged or smeared out in order to end up with an approximately constant pattern of albedo. In order to avoid getting into very complicated analysis, the essential condition is that the units for T, f_n, A and a_n are chosen in such a way that $g(t)$ is approximately constant. Otherwise fig. 3(b) will include significant structures which do not shift towards the point $f = 0$ as T and hence also t increase. For example, if f_n represents the frequency of the 11-year sunspot cycle, then T and $1/f_n$ could preferably be given in years in order to average out the annual and semiannual variations of albedo. Correspondingly A and a_n should each imply incident energy per year over the whole PAS.

But the general picture concerning the form of $g(t)$ to be used is as follows. One can use any form of $g(t)$ if the conditions under consideration necessitate such use. However, use of a significantly variable $g(t)$ must be done in realization of the following caution. If $g(t)$ is significantly variable, the associated amplitude spectrum (corresponding to fig. 3(b)) will consist of different significant structures which do not have common or properly synchronized motions as T and hence t vary. Such a situation complicates the process of deriving expressions for the solar energy amplification factors.

2·2. *The Earth's surface-atmosphere system.* – The Earth's surface-atmosphere system (ESS) may be viewed as a heat engine which receives heat from the Sun at short-wave radiation and thereafter rejects it into space (through the Earth's infrared window) at long-wave radiation. The absorbed short-wave radiation enables the heat engine to do work and hence maintain the ESS weather/climate and related dynamics. About 50% of the short-wave radiation incident onto the ESS is absorbed directly by the Earth's surface. Also about 20% of this incident radiation is absorbed directly by clouds and airborne H_2O, dust, and O_3. It is oceans that provide for 70% of the Earth's surface. We should note that it will take several years for incident short-wave solar radiation to heat up the oceans. This is because of the large heat storage capacity of the oceans, which originates in the fact that the top layer of the oceans circulates and distributes its heat energy. Indeed this is the reason why global distribution of sea surface temperature is not determined in any direct or simple way by the energy balance requirements. The account just given above together with the related account given in the preceding section justify separate treatment or analysis of the long-wave radiation and short-wave radiation expressions in eq. (8) as already done in subsequent parts of the latter section, thus leading to eqs. (9) and (10).

We would like to apply eq. (10) to the Earth's surface-atmosphere system and then obtain a numerical value of Ω_n with f_n representing the frequency of the 11-year sunspot cycle as follows. The solar constant varies by 0.1% over an 11-year sunspot cycle [13,14]. Since f_n is expressed in this case as $1/11$ year^{-1} (see justification in the preceding section) and t is given in years, then the corresponding amplification factor Ω_n is given as

$$\Omega_n \approx 2312 \sin(\pi f_n t)\, e^{-j\pi f_n t}\,, \tag{11}$$

where we have assumed some constant yearly albedo values. Equation (1) gives a maximum value of Ω_n of ~ 2312.

Let us now look at amplification factors corresponding to sunspot cycles with periods longer than that of the 11-year sunspot cycle. From 1723 up to the present time, the most dominant sunspot cycle is that whose period has been varying from ~ 44.3 years (between 1723 and 1768) to the present value of ~ 120.2 years. This particular sunspot cycle (which is drawn in fig. 4 of ref. [5] using thick dashed lines) will hereinafter be referred to as "long-period sunspot cycle" or in short form as "LSC". Sunspot cycles at periods shorter than that of the LSC which existed between 1723 and the present time are the 11-year sunspot cycle, the 22-year sunspot cycle, ... etc. But of all the latter cycles, only the 11-year cycle has been continuously and consistently existing since 1723. We assume (as done in a number of climatology textbooks) that $g(t)$ does not change considerably over an 11-year sunspot cycle. On this basis and as explained in the preceding section, we shall tailor eq. (10) to give Ω_n at the LSC frequency f_n by adopting the following: t is expressed in year units, f_n is expressed in reciprocal of the latter units, A' and a'_n are given in appropriate energy per the latter time unit. Besides, ref. [14] shows that the largest changes in the solar constant for the period since 1750 is estimated to be about 0.1% to 0.4%. On this basis, the mean energy amplification factor Ω_n for the LSC period on the basis of eq. (10) is given as

$$\Omega_n \approx [6915] \sin(\pi f_n t)\, e^{-j\pi f_n t}\,. \tag{12}$$

The last equation gives maximum energy amplification factor of 6915. Relatively larger amplification factors are expected in connection with sunspot cycles whose frequencies are smaller than that of the LSC.

3. – Comparison of observations and the theory in subsect. 2˙2

In this section we would like to see how much available observations agree with the theory given in subsect. 2˙2. The large energy amplification factors given in the latter section obviously imply existence in the Earth's surface-atmosphere system (ESS) of large energy oscillations at frequencies of sunspot cycles. Such large energy oscillations would expectedly be reflected in corresponding variations of temperature and the other weather

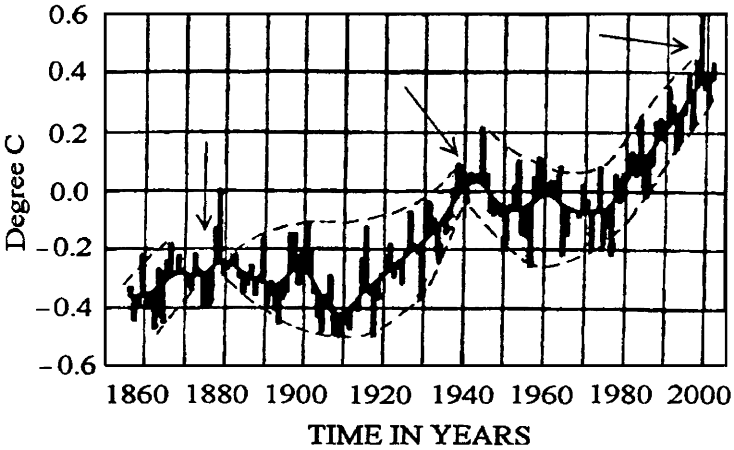

Fig. 6. – A plot of global mean surface temperature over the period 1856-2001 (see ref. [15]). The bars represent annual values as departures from 1961 to 1990 mean. Also the smooth curve shows the result of filtering the annual values to reveal long-term fluctuations. We have used discontinuous lines to sketch out the amplitude-modulation envelopes of the temperature variations using the curve-fitting methods given in ref. [16]. Arrowed lines show locations at which the (sunspot-related) amplitude-modulating oscillations undergo rapid phase reversals (see ref. [17] for details on the extreme right-hand side arrow).

parameters such as rainfall, humidity and air pressure. The good agreement that exists between observations and the theory given in subsect. **2**˙2 is summarized as follows.

a) In line with the theory in subsect. **2**˙2, observation data show that all the major sunspot cycles are significantly reflected in the variations of temperature and other meteorological parameters (*e.g.*, see refs. [2-5, 17, 18]). Some representative illustrations are given in part b) below.

b) The theory presented in sect. **2** (*e.g.*, see eqs. (10), (1) and (12)) shows that sunspot cycles reflected in climatic variations are essentially unstable with time. These sunspot-related cycles (in climatic variations) undergo phase reversals after approximately one complete cycle. Such continuous phase reversals have been commonly established in climatic records (*e.g.*, see figs. 6 and 7 as typical representative examples). Other interesting examples are given in ref. [18] in respect of observed surface temperature in low latitudes (23.6°N–23.6°S) and the southern hemisphere (23.6°–90°S). In fig. 6 the amplitude-modulation envelope is oscillated by an amplitude-modulating oscillation which is anti-phase to the LSC and has a frequency equal to that of the LSC (*e.g.*, see ref. [5]). What is of particular interest here is that the amplitude-modulating oscillation rapidly reverses its phase after approximately one cycle as illustrated in fig. 6. In these phase reversals, the amplitude-modulation envelope changes from a maximum to a node or from a node to a maximum.

In fig. 7 the temperature variations are also shaped into amplitude-modulation envelopes wherein the amplitude-modulating oscillation has a period equal to that of the 11-year sunspot cycle. Note in the figure that the latter oscillation rapidly reverses its phase after approximately one cycle. In these phase reversals, a node

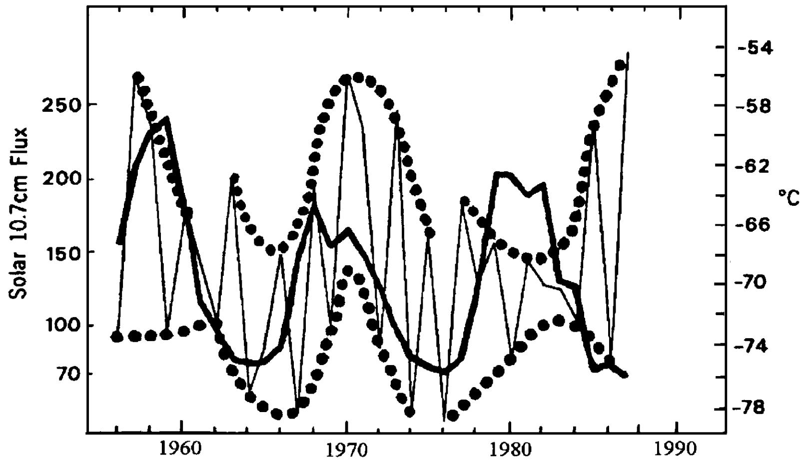

Fig. 7. – Time series of the 10.7 cm solar flux (thick solid lines) in units of 10^{-22} $\mathrm{Wm^{-2}Hz^{-1}}$ and mean 30 mb temperature at the North Pole for all 32 winters from 1956 through 1987 (thin solid lines) as reported by Labitzke and van Loon [19]. We have used dotted lines to map out the amplitude-modulation envelopes of the temperature variations in accordance with the curve-fitting methods given in ref. [16]. Note the phase reversals in the amplitude-modulation envelopes which took place at about the years 1962 and 1975.

rapidly gives way to a maximum or a minimum rapidly gives way to an antinode as illustrated in fig. 7.

c) Phase reversal sequences in sunspot-related climatic oscillations as detailed in sect. **2** have been detected in a large variety of meteorological records and reported in a book by Gnevyshev and Oi [20]. Page 4 of this book reports the following observations concerning the phase reversal sequences mentioned above:

> *Some solar-terrestrial relationships disappear (for some time) almost completely, others change phase, direct relationships being reversed and reverse relationships becoming direct, ...*

Note that the phase reversal sequences mentioned above affect each sunspot-linked climate oscillation and its harmonics. The following two points should be borne in mind concerning the phase reversal sequences. Firstly, the phase reversal points are always along the falling or rising phases of the sunspot-linked energy/temperature oscillation. This ensures that the phase reversal sequences also make the resultant amplitude-modulation envelopes continuously alternate between "sinusoidal" patterns and "node-antinode" patterns as illustrated in figs. 6 and 7. In this way, the phase reversal sequences keep the associated climate system spectrally stirred up in order to avoid situations whereby the system becomes dominantly locked onto a specific, permanently aligned and tuned up spectral pattern. Secondly, simple forward extrapolation of fig. 6 shows that the amplitude-modulation envelope in this figure is expected to phase-reverse itself during the early years of this century and adopt a "node-antinode" pattern with a node as its starting stage. From this node, the pattern is expected to gradually fan out into an antinode at about the year 2023. It is for this reason that the current global warming trend is expected to halt and slightly reverse during the early years of this century. Correspondingly, the roughness or nonlinearity level of global climate is expected to increase gradually as the "node-antinode" pattern fans out to an antinode at about 2023.

d) According to the theory given in sect. **2**, the energy amplification factors associated with sunspot cycles become larger as the periods of the associated sunspot cycles increase. This theoretical conclusion is well supported by observations. For example, a variance spectrum of the Earth's atmospheric temperature during its past history is given in ref. [8]. In this spectrum, the relative variance at the 11-year sunspot cycle period is 1.4 and that at the LSC period is about 3. Also the relative variance at the period of the $\sim$ 2450-year sunspot cycle is 8. This clearly shows that relative variance increases with the period of associated sunspot cycle.

   On the basis of its climatic implications, the fact that the amplification factor on any solar constant perturbation is inversely proportional to the product of the amplitude and frequency of the perturbation (*e.g.*, see eq. (10)) merits further comments and explanation. A deeper and broader look at this fact leads to the following conclusions. As the perturbations approach sufficiently high frequencies, significant amplification occurs only to the sufficiently small perturbations. At the same time, the sufficiently large perturbations are attenuated. But as the perturbations approach sufficiently low frequencies, both small and large perturbations are amplified, although the small perturbations undergo relatively greater amplification. As regards perturbations at medium frequencies, the sufficiently small perturbations are amplified while the relatively large perturbations are attenuated. The general picture gathered here is that the ESS climate is protected or shielded from influences of large and rapid perturbations in the solar constant.

4. – Conclusion

We have presented physical mechanisms through which the tiny variations in the solar constant associated with sunspot cycles are reflected in the ESS in considerably amplified forms. The amplification process involves making a large part of the constant component of Earthward solar energy absorbed into the ESS oscillate more stably at the frequencies of sunspot cycles. Each of the resulting large energy oscillations in the ESS undergoes phase reversal after approximately one period, and also gives rise to corresponding variations in temperature and the other meteorological parameters.

In general, the paper has established (using rigorous theoretical and observational basis) that a planet-atmosphere system (*e.g.*, the ESS) can act as a natural solar energy amplifier as illustrated in fig. 2. This natural amplifier uses internal energy interactions/processing to create or set up conditions by which a large part of the absorbed constant component of incoming solar energy stream oscillates at the frequencies of the tiny solar cycles in the latter stream. In comparison, an electronic amplifier uses a device (*e.g.*, a transistor) to create or set up conditions by which a large part of the constant energy from a power supply (*e.g.*, a battery) is made to oscillate at the frequencies of the relatively small input/incoming signal.

* * *

We are extremely grateful to an anonymous referee whose comments and suggestions have been used to improve an earlier version of the paper into the present version.

REFERENCES

[1] Gray P. E. and Searle C. L., *Electronic Principles* (John Wiley & Sons, New York) 1969.
[2] Njau E. C., *Proc. Indian Nat. Sci. Acad. A*, **66** (2000) 415.
[3] Njau E. C., *Nuovo Cimento C*, **26** (2003) 23.
[4] Njau E. C., *Nuovo Cimento C*, **26** (2003) 613.
[5] Njau E. C., *Nuovo Cimento C*, **27** (2004) 133.
[6] Roden M. S., *Analog and Digital Communication Systems* (Prentice-Hall International, London) 1979.
[7] Taub H. and Schilling D. L., *Principles of Communication Systems* (McGraw-Hill Publishing Company, New York) 1986.
[8] Peixoto J. P. and Oort A., *Physics of Climate* (American Institute of Physics, New York) 1992.
[9] Tandberg-Hanssen E., *Solar Activity* (Blaisdell Publishing Company, London) 1967.
[10] Cox A. N., Livingston W. C. and Matthews M. S. (Editors), *Solar Interior and Atmosphere* (The University of Arizona Press, Tucson) 1991.
[11] Fath E. A., *The Elements of Astronomy* (McGraw-Hill Book Company, New York) 1955.
[12] Struve O., Lynds B. and Pillans H., *Elementary Astronomy* (Oxford University Press, New York) 1959.
[13] Phillips K. J. H., *Guide to the Sun* (Cambridge University Press, Cambridge) 1995.
[14] Pap J. M., Forhlich C., Hudson H. S. and Solanki S. K. (Editors), *The Sun as a Variable Star* (Cambridge University Press, Cambridge) 1993.
[15] TIEMPO, Issue 43 (March 2002)26.
[16] The curve-fitting toolbox at `www.mathworks.com/nncurvefitting` visited on 21/10/2004.
[17] Njau E. C., to be published in *Int. J. Renewable Energy* (2004).
[18] Njau E. C., *Int. J. Renewable Energy*, **17** (1999) 319.
[19] Labitzke K. and Van Loon H., *J. Atmos. Terr. Phys.*, **50** (1988) 197.
[20] Gnevyshev M. N. and Oi A. I. (Editors), *Effects of Solar Activity on the Earth's Atmosphere and Biosphere* (Israel Program for Scientific Translations, Jerusalem) 1977.